THE JOURNAL OF PHYSICAL CHEMISTRY C

Subscriber access provided by Universitätsbibliothek Bern

C: Physical Processes in Nanomaterials and Nanostructures

Microscopic Approach to the Problem of Cooperative Spin Crossover in Polynuclear Cluster Compounds. Application to Tetranuclear Iron(II) Square Complexes

Serghei M. Ostrovsky, Andrew V. Palii, Silvio Decurtins, Shi-Xia Liu, and Sophia I. Klokishner

J. Phys. Chem. C, **Just Accepted Manuscript** • DOI: 10.1021/acs.jpcc.8b05599 • Publication Date (Web): 31 Aug 2018

Microscopic Approach to the Problem of Cooperative Spin Crossover in Polynuclear Cluster Compounds. Application to Tetranuclear Iron(II) Square Complexes.

S. Ostrovsky,[1*] A. Palii,[1,2] S. Decurtins,[3] S.-X. Liu[3] and S. Klokishner[1*]

[1] *Department of Physics of Semiconductor Compounds "Sergiu Radauțan", Institute of Applied Physics, Kishinev, Moldova, MD-2028*

[2] *Department of Molecular Magnetic Nanomaterials, Institute of Problems of Chemical Physics, Chernogolovka, Moscow Region, Russia, 142432*

[3]*Departement für Chemie und Biochemie, Universität Bern, Freiestrasse 3, CH-3012 Bern, Switzerland*

[*]Corresponding authors: klokishner@yahoo.com, sm_ostrovsky@yahoo.com,

Abstract

A new microscopic approach to the problem of cooperative spin crossover in molecular crystals containing polynuclear complexes as structural units has been developed. The cooperative intercluster interaction in the crystal is shown to arise from the coupling of the molecular modes to the acoustic phonons. The interaction between ions, which belong to the same cluster, is also taken into account, that leads to interesting features in the temperature dependence of the magnetic susceptibility which are not observed in mononuclear molecular crystals. The developed general approach is adapted to the case of tetranuclear square complexes. In the latter the effect of intracluster interactions on the type of the spin transition is analyzed. The applicability of the developed approach is illustrated by the interpretation of the experimental data on the spin transition in the tetranuclear $[Fe(tpa)\{N(CN)_2\}]_4\cdot(BF_4)_4\cdot(H_2O)_2$ cluster compound. For this compound the theory well reproduces the observed two-step spin transition with the plateau between the steps that corresponds to the cluster configuration with 2 high spin Fe(II) ions located along the diagonal of the square.

1. Introduction

The spin crossover (SCO) phenomenon was discovered in the early 1930s when Cambi and co-workers reported the unusual magnetic behavior of some iron(III) complexes. [1-4] Since that time hundreds of SCO compounds have been synthesized and characterized. The SCO phenomenon attracts broad current interest due to the wide range of potential applications in

molecular electronics and spintronics [5-11] and it is in the focus of many experimental and theoretical studies (for details see [12,13] and reference therein). SCO can be induced not only by temperature but also by light. In [14] it was demonstrated that a quantitative light-induced spin transition can be achieved for transparent crystalline samples.

Since the interaction between SCO ions belonging to the same cluster can play an important role in the enhancing of bistable behavior, researchers turned their attention to polynuclear cluster compounds. The spin transition in cluster compounds can possess some peculiarities not observed in mononuclear SCO complexes. For example, it can take place in several steps. The first two-step SCO in binuclear complex was reported in [15]. The presence of the second step in the temperature dependence of the magnetic behavior of the $[Fe(bt)(NCS)_2]_2$bpym complex was explained by the intercenter Coulomb interaction between Fe ions. Later on, other binuclear SCO complexes have been synthesized and characterized. A comprehensive review of the experimental work on dinuclear SCO compounds can be found in [16,17]. Another type of polynuclear SCO compounds, attracting interest of researchers last years, includes tetranuclear iron square complexes.[18-23] A variety of magnetic behavior is found in these systems: (i) one-step transition between the configuration with two low-spin (*ls*) and two high-spin (*hs*) ions located along the side of the square and configuration with all 4 Fe ions in the *hs* state [18]; (ii) two-step spin transition with the first step corresponding to the transition between the configuration with all four Fe ions in the *ls* state and the configuration with three *ls* and one *hs* ion and the second step being between the 3 *ls* + 1 *hs* configuration and that with 2 *ls* and 2 *hs* ions located along the diagonal of the square [19]; (iii) two-step spin transition between the configurations with all four Fe ions in the *ls* state and all Fe ions in the *hs* state with the plateau between steps corresponding to the configuration with two *ls* and two *hs* ions located along the diagonal of the square.[21] It should also be mentioned that in papers [18-21] besides the type of the SCO transition in tetranuclear square complexes the role of intracluster exchange interaction between the *hs*-Fe^{II} ions is qualitatively discussed. It is pointed out that in the $[Fe_4(HL^1)_4](BF_4)_4 \bullet (H_2O)_2 \bullet CH_3OH$ compound[18] only two iron(II) ions participate in the $ls \rightarrow hs$ transformation, while the other two are in the *hs* state in the whole temperature range. Namely, the exchange interaction between the latter ones is assumed to be responsible for the increase of the χT product in the low temperature range. As follows from the structural , magnetic susceptibility and Mössbauer data for the compound reported in [19] the effect of exchange interaction can only manifest at temperatures above 300 K, when two of the four Fe^{II} ions become high-spin. However, this effect is small as compared with that of cooperative interactions since in spin crossover compounds the exchange parameter is usually of the order of few wavenumbers.

It should be also mentioned that recently the family of pyrazolate-based [2x2] Fe^{II}_4 grid compounds has been significantly expanded with the aid of the compartmental proligand HL^{Br}.[22] Six all-ferrous compounds $[Fe^{II}_4L^{Br}_4]X_4$ obtained in [22] have been characterized structurally and magnetically. It has been shown that in the crystalline material the spin state varies from 4 hs via the 3hs-1ls to the 2hs-2ls forms, with some grids demonstrating thermal SCO. In [23] it has been demonstrated that the spin state of the Fe^{II} sites and the magnetic properties of a [2x2] Fe^{II} grid-like complex can be varied by the change of the degree of deprotonation of the hydrazine-based N-H sites of the ligand in the complex.

The SCO transformation in solids is essentially a cooperative phenomenon. There are two general trends in the description of the cooperative SCO, namely, the macroscopic and microscopic theoretical approaches. Within the framework of macroscopic treatments the driving force of spin transition is the elastic interaction, the strength of which depends on the electronic state (*hs* or *ls*) of the SCO center. Among the various macroscopic models used for the interpretation of experimental data there are the thermodynamic approach [24-26], the Wainflasz and Pick model [27] and its extensions called "Ising-like models" [28-38], atom-phonon coupling model [39-42] and mechano-elastic model.[43-46] In molecular crystals the elasticities of intra- and intermolecular spaces are different that has been taken into account in the model suggested in[47,48] and applied for the description of the SCO phenomena in mononuclear [49, 50] and polynuclear [51-53] molecular crystals. The first microscopic approach to the description of cooperative SCO was proposed by Sasaki and Kambara.[54-56] In their model the coupling between electronic shells of SCO metal ions takes place via the phonon field giving rise to cooperative interaction in the whole crystal. A review of the existing theoretical models for the description of the SCO phenomenon can be found in [57].

In molecular crystals each SCO ion participates both in molecular (local) vibrations and in the vibrations propagating along the crystal (phonons). The energy pattern of each SCO ion is formed by the interaction with molecular vibrations, while the cooperativity in the whole crystal arises from the electron-phonon interaction. Recently, this specific feature of molecular crystals has been accounted for in a new microscopic theoretical approach to the description of SCO phenomenon in molecular crystals containing mononuclear [58] and binuclear [59] fragments as structural elements. In the present contribution this microscopic approach is generalized to the case of molecular crystals containing clusters of arbitrary nuclearity and applied to the description of SCO phenomenon in Fe^{II}_4 square complexes.

2. Model

2.1. Crystal Hamiltonian

The detailed description of the new microscopic theoretical approach to the problem of SCO can be found in our previous papers where it was applied to the description of spin transitions in crystals containing mononuclear [58] and binuclear [59] structural units. Here we generalize the suggested approach to the case of crystals consisting of clusters of arbitrary nuclearity. With this aim we briefly describe the main points of our model reported in [58,59] paying special attention to the changes that should be introduced in the model to make it suitable for the description of the compounds containing polynuclear SCO clusters.

The crystal Hamiltonian is presented as

$$H = H_0 + H_{\text{int}} + H_{ph}, \qquad (1)$$

where H_0 is the Hamiltonian of non-interacting clusters, H_{int} is the cooperative interaction between the clusters and H_{ph} is the Hamiltonian of free phonons.

The Hamiltonian H_0 in general looks as follows

$$\begin{aligned} H_0 = & \sum_{\boldsymbol{n}} \sum_{\substack{i=1\ldots m \\ p=1\ldots 15}} \left\{ \frac{\hbar\omega_{ls}^{p}}{2} \left[\left(x_{\boldsymbol{ni}}^{ls,p} \right)^2 - \frac{\partial^2}{\partial \left(x_{\boldsymbol{ni}}^{ls,p} \right)^2} \right] + \upsilon_{ls}^{p}\, x_{\boldsymbol{ni}}^{ls,p} \right\} \hat{\tau}_{\boldsymbol{ni}}^{ls} \\ & + \sum_{\boldsymbol{n}} \sum_{\substack{i=1\ldots m \\ p=1\ldots 15}} \left\{ \Delta_{hs,ls} + \frac{\hbar\omega_{hs}^{p}}{2} \left[\left(x_{\boldsymbol{ni}}^{hs,p} \right)^2 - \frac{\partial^2}{\partial \left(x_{\boldsymbol{ni}}^{hs,p} \right)^2} \right] + \upsilon_{hs}^{p}\, x_{\boldsymbol{ni}}^{hs,p} \right\} \hat{\tau}_{\boldsymbol{ni}}^{hs} \\ & + \sum_{\boldsymbol{n}} \sum_{\substack{f_i = hs,ls \\ (i=1\ldots m)}} U(f_1 \ldots f_m) \hat{\tau}_{\boldsymbol{n}1}^{f_1} \ldots \hat{\tau}_{\boldsymbol{n}m}^{f_m}, \end{aligned} \qquad (2)$$

here $\boldsymbol{n}$ is the vector that labels the clusters in the crystal, the index i enumerates the SCO ions in each cluster, the vector $\boldsymbol{ni} = \boldsymbol{n} + \boldsymbol{Ri}$ determines the position of the i-th SCO ion in the $\boldsymbol{n}$-th cluster. A crystal cell is assumed to contain one cluster with an arbitrary number of SCO ions. There are no restrictions on the cluster symmetry. The diagonal matrices $\hat{\tau}_{ni}^{ls}$ and $\hat{\tau}_{ni}^{hs}$ of the dimension $\left(g_{ls} + g_{hs}\right)^m$ (with m being the number of SCO ions in the cluster) possess the following non-vanishing matrix elements $\left\langle \psi_{\boldsymbol{ni}}^{hs}\left(\mu_{hs}\right) \middle| \tau_{\boldsymbol{ni}}^{hs} \middle| \psi_{\boldsymbol{ni}}^{hs}\left(\mu_{hs}\right) \right\rangle = 1$ and $\left\langle \psi_{\boldsymbol{ni}}^{ls}\left(\mu_{ls}\right) \middle| \tau_{\boldsymbol{ni}}^{ls} \middle| \psi_{\boldsymbol{ni}}^{ls}\left(\mu_{ls}\right) \right\rangle = 1$, where $\mu_{hs} = 1, 2, \ldots g_{hs}$ and $\mu_{ls} = 1, 2, \ldots g_{ls}$ numerate the *hs* and *ls* states. The first two terms in Eq.(2) describe the free cluster vibrations and the electron-vibrational interaction in the *ls* and *hs* states. In fact Eq. (2) accounts for all 15 normal local vibrational modes inherent to complexes consisting of a central metal ion and six nearest ligands. Respectively, $x_{\boldsymbol{ni}}^{ls,p}$ and $x_{\boldsymbol{ni}}^{hs,p}$ are the symmetric displacements of the nearest surrounding of the i-th SCO ion in the n-th cluster in the *ls* and *hs* states that correspond to all above mentioned modes with ω_{ls}^{p} and ω_{hs}^{p} being the frequencies of these modes. Since in the majority of the

examined Fe(II) SCO complexes the *ls* to *hs* transition is not accompanied by a change in the crystal symmetry, the interaction of the SCO centers with the full-symmetric breathing vibrations turns out to be mainly responsible for the spin transition. Therefore, further on in equation (2) we keep only the vibronic coupling constants $\upsilon_{ls}^{A_1}$ and $\upsilon_{hs}^{A_1}$ different from zero. In the subsequent consideration for the sake of simplicity the superscript A_1 is omitted in the notation of these coupling constants, of the frequencies of the full symmetric molecular vibrations as well as in the corresponding symmetric displacements. Finally, $\Delta_{hs,ls}$ is the crystal field energy gap between the examined states.

The last term in Eq.(2) is introduced in order to take into account the specific feature of cluster compounds and, namely, the presence of the interactions between ions belonging to the same cluster. Among these interactions the intracluster Coulomb interaction, the interaction arising from the mixing of the ground and charge transfer excited states by electron transfer [59] as well as the interaction via the field of optic phonons can be mentioned. These intracluster interactions between the SCO ions affect the energies of all cluster configurations. The additional contribution to the energy gap $m\Delta_{hs,ls}$ between the configuration with all ions in the *hs* state ($n = m$ with n being the number of ions in the cluster in *hs* configuration) and the configuration with all ions in the *ls* state ($n = 0$) that comes from the intracluster interaction redetermines this gap. In all subsequent calculations the effective gap $\Delta = m\Delta_{hs,ls} + U(\text{all } hs) - U(\text{all } ls)$ is used, where $U(\text{all } hs)$ and $U(\text{all } ls)$ denote the energies of interactions between the cluster ions when all of them are in the *hs*- or *ls*-states, respectively. As for the energies of other cluster configurations (with $n = 1, 2 \ldots m\text{-}1$), they become not equidistant on the account of the intracluster interactions, and it is convenient to describe them using the energy shifts from the equidistant positions $n\Delta / m$. The corresponding shifts are denoted as δ_n^i (the superscript i is introduced since the cluster configurations with the same number of *hs* ions can have different energies depending on the mutual arrangement of the ions in the *hs* and *ls* states). The explicit form of the parameters δ_n^i depends on the type of the SCO ions, the geometry and symmetry of the cluster under examination. This fact is demonstrated in the subsequent sections wherein within the framework of the suggested model the origin of the spin transition in the Fe_4^{II} squares is discussed.

The Hamiltonian of cooperative interaction H_{int} employed in the model is obtained in the framework of the approach suggested by Hizhnyakov and coworkers [60,61] for a single impurity center. The key statement underlying this approach is that the ligand surrounding of the metal ion participates in two types of vibrations, namely, in the local vibrations and (to less extent) in

the vibrations propagating along the crystal (phonons). Under this assumption the symmetry adapted ligand displacements of the metal ion surrounding (configurational coordinates) are presented as a linear superposition of the normal coordinates of the local modes and phonons of the same symmetry, with the main contribution being given by the local modes. The weight with which each of the mentioned vibrations enters in the resulting one is characterized by the dimensionless parameter λ of the model. This presentation of the configurational coordinates introduced in [60,61] can be justified by the fact that in real molecular crystals such as SCO ones the main contribution to the interaction with vibrations comes from few local or pseudolocal vibrations; while the contribution of phonons to this interaction is much smaller. Thus, the linear interaction of the SCO center with phonons, which is proportional to λ, is weak in molecular crystals and it is not taken into account as in [60-62]. At the same time the latter interaction is also very important since it is responsible for the relaxation of the excited states. In the accepted approach, besides the linear coupling of electrons to the molecular (local) vibrational coordinate, the interaction Hamiltonian for a single ion contains an additional bilinear term proportional to λ as well as to the product of normal coordinates of crystal vibrations and the coordinate of the molecular vibration.[60,61] In the general case of a crystal containing SCO polynuclear clusters as structural units, this term can be written as:

$$H_{\text{int}} = -\sum_{\boldsymbol{n},\boldsymbol{n}'} \sum_{\boldsymbol{\kappa}\nu} \sum_{i,j=1\ldots m} \frac{1}{\hbar\omega_{\boldsymbol{\kappa}\nu}} \varphi_{\boldsymbol{\kappa}\nu}^{\boldsymbol{n}i} \varphi_{\boldsymbol{\kappa}\nu}^{\boldsymbol{n}'j*} \exp\left[i\boldsymbol{\kappa}\left(\boldsymbol{n}i - \boldsymbol{n}'j\right)\right], \tag{3}$$

where the values $\varphi_{\boldsymbol{\kappa}\nu}^{\boldsymbol{n}i}$ are

$$\varphi_{\boldsymbol{\kappa}\nu}^{\boldsymbol{n}i} \equiv \varphi_{\boldsymbol{\kappa}\nu}^{\boldsymbol{n}i}\left(\mathrm{A}_1\right) = -\lambda \frac{\hbar}{\sqrt{2Nm\omega_{\boldsymbol{\kappa}\nu}}} \left[\frac{1}{\sqrt{\omega_{hs}}} \tau_{hs}^{ni} x_{hs}^{ni} \left(\omega_{hs}^2 - \omega_{\boldsymbol{\kappa}\nu}^2\right) + \frac{1}{\sqrt{\omega_{ls}}} \tau_{ls}^{ni} x_{ls}^{ni} \left(\omega_{ls}^2 - \omega_{\boldsymbol{\kappa}\nu}^2\right) \right] f_{\boldsymbol{\kappa}\nu}\left(\mathrm{A}_1\right), \tag{4}$$

with $\omega_{\boldsymbol{\kappa}\nu}$ and $f_{\boldsymbol{\kappa}\nu}\left(\mathrm{A}_1\right)$ being ,respectively, the phonon frequency and the Van-Vleck coefficients.[63-65] The latter perform the unitary transformation from the full symmetric displacements of the ligand environments of the metal ions to the crystal normal coordinates , ν numerates the phonon modes.

For the subsequent calculations it is convenient to exclude from Eq.(3) the interactions between the SCO ions belonging to the same cluster.[59] It can be done under the assumption that the dominant contribution to the overall cooperative effect is produced by the long-wave acoustic phonons. Within this approximation the strength of each interionic interaction in H_{int} becomes independent of the distance between the two SCO ions. In this case the finite number of elastic interactions of a SCO ion with the ions belonging to the same cluster can be neglected as

compared with the infinite number of interactions with all other ions in the crystal. As a result, Eq.(3) can be rewritten as:

$$H_{\text{int}} = -\frac{1}{2}\sum_{\substack{\boldsymbol{n},\boldsymbol{n}' \\ \boldsymbol{n}\neq\boldsymbol{n}'}} \sum_{i,j=1\ldots m} \Big[J^{hs,hs}\left(\boldsymbol{n}\,i-\boldsymbol{n}'j\right)\tau_{\boldsymbol{n}i}^{hs}\,x_{\boldsymbol{n}i}^{hs}\tau_{\boldsymbol{n}'j}^{hs}\,x_{\boldsymbol{n}'j}^{hs} + J^{ls,ls}\left(\boldsymbol{n}\,i-\boldsymbol{n}'j\right)\tau_{\boldsymbol{n}i}^{ls}\,x_{\boldsymbol{n}i}^{ls}\tau_{\boldsymbol{n}'j}^{ls}\,x_{\boldsymbol{n}'j}^{ls} + 2J^{hs,ls}\left(\boldsymbol{n}\,i-\boldsymbol{n}'j\right)\tau_{\boldsymbol{n}i}^{hs}\,x_{\boldsymbol{n}i}^{hs}\tau_{\boldsymbol{n}'j}^{ls}\,x_{\boldsymbol{n}'j}^{ls} \Big], \tag{5}$$

where $\boldsymbol{n} \neq \boldsymbol{n}'$ since the coupling of the ions inside each cluster is excluded. In this case the parameters $J^{f,f'}\left(\boldsymbol{n}\,i-\boldsymbol{n}'j\right)$ look as follows:

$$J^{f,f'}\left(\boldsymbol{n}\,i-\boldsymbol{n}'j\right) = \frac{\pi\lambda^2\,\hbar\,R_f R_{f'}}{6\,c^2 N m\sqrt{\omega_f\omega_{f'}}}\left[16\,\omega_f^2\,\omega_{f'}^2 - 8\left(\omega_f^2+\omega_{f'}^2\right)\omega_M^2 + 5\,\omega_M^4\right], \tag{6}$$

where f = *hs* or *ls* and ω_M is the Debye frequency.

Finally, the Hamiltonian of free phonons is

$$H_{ph} = \sum_{\boldsymbol{\kappa}\nu}\hbar\omega_{\boldsymbol{\kappa}\nu}\left(a_{\boldsymbol{\kappa}\nu}^{+}a_{\boldsymbol{\kappa}\nu} + 1/2\right). \tag{7}$$

with $a_{\boldsymbol{\kappa}\nu}^{+}$ and $a_{\boldsymbol{\kappa}\nu}^{+}$ being the phonon creation and annihilation operators.

2.2. Mean Field Approximation

To reduce the problem of interacting clusters (Eq.(5)) to the one cluster problem, the mean field approximation is used (for details see [58,59]). The eigenvalues of the Hamiltonian (Eq.(1)) look as

$$E_{n,\{k_l^p\}}^{i}\left(\overline{\tau^{ls}x^{ls}},\overline{\tau^{hs}x^{hs}}\right) = E_n^i\left(\overline{\tau^{ls}x^{ls}},\overline{\tau^{hs}x^{hs}}\right) + \sum_{l=m-n+1}^{m}\sum_{p=1\ldots15}\hbar\omega_{ls}^{p}\left(k_l^p+\tfrac{1}{2}\right) + \sum_{l=1}^{n}\sum_{p=1\ldots15}\hbar\omega_{hs}^{p}\left(k_l^p+\tfrac{1}{2}\right), \tag{8}$$

where

$$E_n^i\left(\overline{\tau^{ls}x^{ls}},\overline{\tau^{hs}x^{hs}}\right) = \frac{\Delta}{m}n - \delta_n^i - \frac{m-n}{2\hbar\omega_{ls}}\left(\upsilon_{ls} - J^{ls,ls}\,\overline{\tau^{ls}x^{ls}} - J^{hs,ls}\overline{\tau^{hs}x^{hs}}\right)^2 - \frac{n}{2\hbar\omega_{hs}}\left(\upsilon_{hs} - J^{hs,hs}\,\overline{\tau^{hs}x^{hs}} - J^{hs,ls}\,\overline{\tau^{ls}x^{ls}}\right)^2 \tag{9}$$

In this equation k_l^p are the vibrational quantum numbers determining the energies of the *m*-dimensional harmonic oscillator that correspond to the normal *p*-mode and the zero energy is chosen as the energy of the configuration, where all spin crossover ions are in the *ls* state and the effect of the vibronic and cooperative interactions is neglected. The intercenter mean field

parameters $J^{f,f'} = \sum_{\boldsymbol{n}',i,j} J^{f,f'}\left(\boldsymbol{n}i - \boldsymbol{n}'j\right)$ (*f*, *f'* = *hs* or *ls*) are independent of the SCO ion position in the crystal and take on the form [58,59]

$$J^{f,f'} = \frac{\pi\lambda^2 \hbar R_f R_{f'}}{6\,c^2\sqrt{\omega_f \omega_{f'}}}\left[16\,\omega_f^2\,\omega_{f'}^2 - 8\left(\omega_f^2 + \omega_{f'}^2\right)\omega_M^2 + 5\,\omega_M^4\right]. \tag{10}$$

The order parameters $\overline{\tau^{ls}x^{ls}}$ and $\overline{\tau^{hs}x^{hs}}$ are obtained by statistical averaging of the corresponding operators and obey the following system of transcendental equations:

$$\overline{\tau^{ls}x^{ls}} = -\frac{1}{Z\left(\overline{\tau^{ls}x^{ls}},\ \overline{\tau^{hs}x^{hs}}\right)\hbar\omega_{ls}}\left(\upsilon_{ls} - J^{ls,ls}\,\overline{\tau^{ls}x^{ls}} - J^{hs,ls}\overline{\tau^{hs}x^{hs}}\right)$$
$$\times\sum_{n=0}^{m}\ \frac{m-n}{m}N_n^i\frac{\left(g_{ls}\right)^{m-n}\left(g_{hs}\right)^n}{\prod\limits_{p=1\ldots15}2^m\sinh^{m-n}\left(\frac{\hbar\omega_{ls}^p}{2\,k_BT}\right)\sinh^n\left(\frac{\hbar\omega_{hs}^p}{2\,k_BT}\right)}\exp\left(-\frac{E_n^i}{k_BT}\right),$$

$$\overline{\tau^{hs}x^{hs}} = -\frac{1}{Z\left(\overline{\tau^{ls}x^{ls}},\ \overline{\tau^{hs}x^{hs}}\right)\hbar\omega_{hs}}\left(\upsilon_{hs} - J^{hs,hs}\,\overline{\tau^{hs}x^{hs}} - J^{hs,ls}\overline{\tau^{ls}x^{ls}}\right)$$
$$\times\sum_{n=0}^{m}\ \frac{n}{m}N_n^i\frac{\left(g_{ls}\right)^{m-n}\left(g_{hs}\right)^n}{\prod\limits_{p=1\ldots15}2^m\sinh^{m-n}\left(\frac{\hbar\omega_{ls}^p}{2\,k_BT}\right)\sinh^n\left(\frac{\hbar\omega_{hs}^p}{2\,k_BT}\right)}\exp\left(-\frac{E_n^i}{k_BT}\right). \tag{11}$$

In eq.(11) N_n^i denotes the number of equivalent configurations with *n hs* and (*m*-*n*) *ls* ions. The partition function has the following form:

$$Z\left(\overline{\tau^{ls}x^{ls}},\ \overline{\tau^{hs}x^{hs}}\right) = \sum_{n=0}^{m}\ N_n^i\frac{\left(g_{ls}\right)^{m-n}\left(g_{hs}\right)^n}{\prod\limits_{p=1\ldots15}2^m\sinh^{m-n}\left(\frac{\hbar\omega_{ls}^p}{2\,k_BT}\right)\sinh^n\left(\frac{\hbar\omega_{hs}^p}{2\,k_BT}\right)}\exp\left(-\frac{E_n^i}{k_BT}\right). \tag{12}$$

As it was already pointed out, in these equations ω_f and υ_f (*f*=*hs*,*ls*) correspond to the full symmetric vibrations. The presented above model is general and can be applied to cluster compounds with an arbitrary number of SCO ions in the cluster. In the model there are no limitations on the symmetry and structure of the cluster.

2.3. Spin Crossover in Fe_4^{II} Squares

In this subsection the general model presented above is adapted to the case of tetranuclear square complexes containing 4 SCO iron(II) ions. An isolated tetranuclear cluster as a whole possesses the following electronic configurations: (i) *ls*-*ls*-*ls*-*ls* (all four Fe^{II} ions are in *ls* state,

one configuration of the cluster, $N_0 = 1$); (ii) *hs-ls-ls-ls* (one *hs* and three *ls* ions, four possible configurations of the cluster that differ in the position of the *hs* ion, $N_1 = 4$); (iii) *hs-hs-ls-ls* (two *hs* and two *ls* ions with *hs* ions situated in the neighboring corners of the square, four possible configurations of the cluster, $N_2^s = 4$); (iv) *hs-ls-hs-ls* (two *hs* and two *ls* ions with *hs* ions situated on the corners of the square along its diagonal, two possible configurations of the cluster, $N_2^d = 2$); (v) *hs-hs-hs-ls* (one *ls* and three *hs* ions, four possible configurations of the cluster that differ in the position of the *ls* ion, $N_3 = 4$); and (vi) *hs-hs-hs-hs* (all four Fe^{II} ions are in *hs* state, one configuration of the cluster, $N_4 = 1$). All mentioned electronic configurations of the tetranuclear square cluster are illustrated in Fig.1.

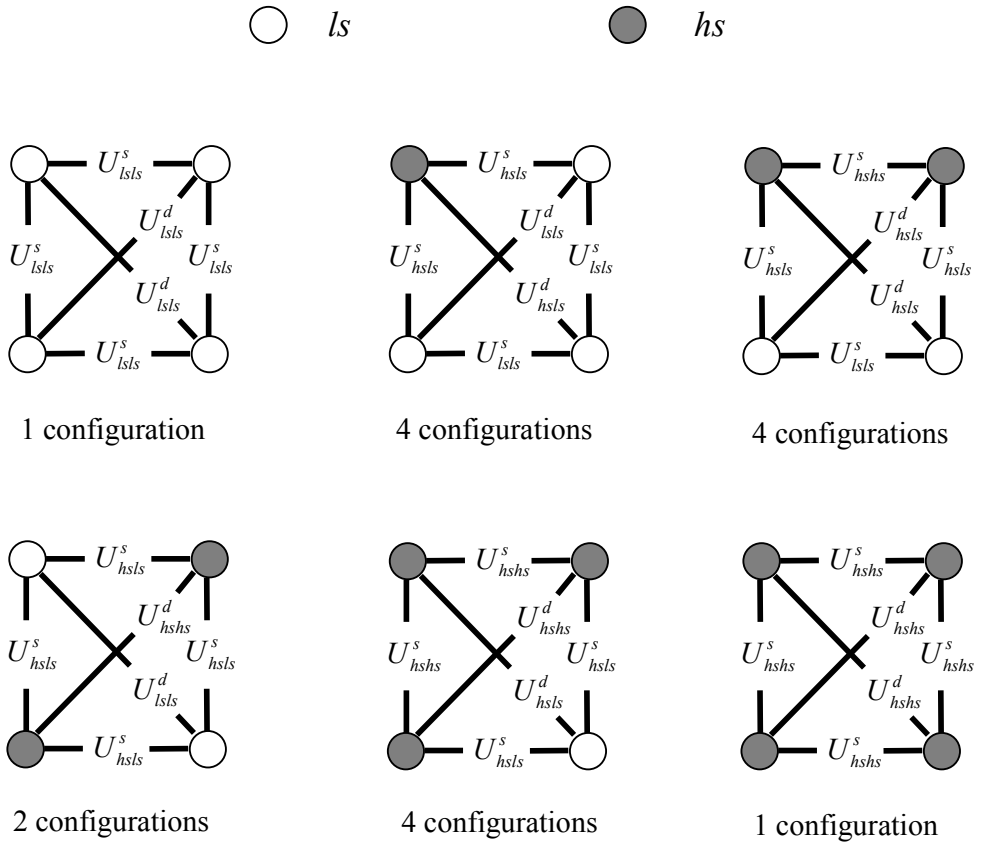

Fig.1. Possible electronic configurations of the tetranuclear square SCO cluster. For each configuration different types of pair interactions are schematically shown.

All equations obtained in Section 2.2 can be applied to the examination of the tetranuclear square clusters (Fig.1) by setting *m*=4. However, the explicit form of $\delta^i_{n_{hs}}$ parameters should be

specified. The last term in Eq.(2) represents the sum of pair interactions between all SCO ions in the cluster. In the subsequent consideration the total energies of these interion interactions are denoted as U_{ij}^{l}, where subscripts *i*, *j* describe the types of interacting ions (*hs* or *ls*) and the superscript *l* is used to differentiate between the location of interacting ions (along the side or the diagonal of the square). All possible two-center interactions between the ions situated along the sides and the diagonals of the square cluster are illustrated in Fig.1. The parameters $U\left(f_1 f_2 f_3 f_4\right)$ for each electronic configuration presented in Fig.1 can be expressed in terms of U_{ij}^{l} parameters as follows:

$$U\left(ls\text{-}ls\text{-}ls\text{-}ls\right) = 4U_{lsls}^{s} + 2U_{lsls}^{d},$$

$$U\left(hs\text{-}ls\text{-}ls\text{-}ls\right) = 2U_{lsls}^{s} + 2U_{hsls}^{s} + U_{lsls}^{d} + U_{hsls}^{d},$$

$$U\left(hs\text{-}hs\text{-}ls\text{-}ls\right) = U_{lsls}^{s} + U_{hshs}^{s} + 2U_{hsls}^{s} + 2U_{hsls}^{d},$$

$$U\left(hs\text{-}ls\text{-}hs\text{-}ls\right) = 4U_{hsls}^{s} + U_{lsls}^{d} + U_{hshs}^{d},$$

$$U\left(hs\text{-}hs\text{-}hs\text{-}ls\right) = 2U_{hshs}^{s} + 2U_{hsls}^{s} + U_{hshs}^{d} + U_{hsls}^{d}, \qquad (13)$$

$$U\left(hs\text{-}hs\text{-}hs\text{-}hs\right) = 4U_{hshs}^{s} + 2U_{hshs}^{d},$$

where superscripts *s*, *d* refer to the ions located along the side or diagonal of the square, respectively. Due to intracluster interactions the energy gap between the configurations *ls*-*ls*-*ls*-*ls* and *hs*-*hs*-*hs*-*hs* looks as follows $\Delta = 4\Delta_{hs,ls} + U\left(hs\text{-}hs\text{-}hs\text{-}hs\right) - U\left(ls\text{-}ls\text{-}ls\text{-}ls\right)$. The energy shifts from the equidistant positions $n\Delta/4$ for other cluster configurations (with 1, 2 or 3 *hs* ions) can be found from Eq.(13) as

$$\delta_1 = \delta_s + \tfrac{1}{2}\delta_d,\ \delta_2^s = \delta_s + \delta_d,\ \delta_2^d = 2\delta_s,\ \delta_3 = \delta_s + \tfrac{1}{2}\delta_d \qquad (14)$$

with

$$\delta_{s(d)} = U_{hshs}^{s(d)} + U_{lsls}^{s(d)} - 2U_{hsls}^{s(d)},$$

where the parameters $\delta_1, \delta_2^s, \delta_2^d$ and δ_3 refer to the cluster configurations *hs*-*ls*-*ls*-*ls*, *hs*-*hs*-*ls*-*ls*, *hs*-*ls*-*hs*-*ls* and *hs*-*hs*-*hs*-*ls*, respectively. As can be seen from Eq.(14), the effect of intracluster interaction between the SCO ions in tetranuclear square clusters can be described with only two parameters δ_s and δ_d.

3. Analysis of the experimental results

3.1. Evaluation of intra- and intercenter parameters

We start with the estimation of the vibronic coupling constants υ_{ls} and υ_{hs} characterizing the interaction of a single SCO Fe^{II}- ion in its *ls* $^1A_1$ and *hs* $^5T_2$ states with the local full symmetric breathing mode. The operator of interaction with this mode for a complex of cubic symmetry can be presented in the form of the derivative of the cubic crystal field potential with respect to metal-ligand distances and the coupling parameters for SCO Fe^{II} ions can be expressed as [58]

$$\upsilon_{ls} = 120\sqrt{\frac{\hbar\omega_{ls}}{6f_{ls}}}\frac{Dq_{ls}}{R_{ls}},\ \upsilon_{hs} = 20\sqrt{\frac{\hbar\omega_{hs}}{6f_{hs}}}\frac{Dq_{hs}}{R_{hs}}. \qquad (15)$$

The typical values of the force constants and the cubic crystal field parameters in the *hs*- and *ls* states of the Fe^{II}-ion can be found in [58,66] and are $f_{hs} = 7.95 \cdot 10^4$ cm^{-1}/Å^2, $f_{ls} = 1.14 \cdot 10^5$ cm^{-1}/Å^2, $Dq_{hs} = 1176$ cm^{-1}, $Dq_{ls} = 2055$ cm^{-1}. The average metal-ligand distances in the *ls*- and *hs*-states are equal to $R_{ls} = 2$ Å and $R_{hs} = 2.2$ Å. The frequencies of all 15 normal modes for the FeN_6 fragment are taken from [67], where the vibrational spectrum of the SCO $[Fe(phen)_2(NCS)_2]$ complex was examined with the aid of different experimental techniques and DFT calculations. For the full symmetric vibrations the corresponding values are $\hbar\omega_{hs} = 97$ cm^{-1} and $\hbar\omega_{ls} = 151$ cm^{-1}. [67] Substituting these values into Eq.(15) one finds $\upsilon_{hs} = 152$ cm^{-1} and $\upsilon_{ls} = 1832$ cm^{-1}. The parameters of intercenter interactions $J^{ls,ls}$, $J^{hs,hs}$ and $J^{hs,ls}$ are evaluated with the aid of Eq.(10). In this estimation for the parameters $\hbar\omega_{hs}$, $\hbar\omega_{ls}$, R_{hs} and R_{ls} we use the same values as those above taken for the calculation of the vibronic coupling constants. For the speed of sound and the mean value of the maximal frequency (identified here with the Debye frequency) the values $c \approx 2 \cdot 10^5$ cm/s [68] and $\hbar\omega_M = 23$ cm^{-1} [66] characteristic for spin crossover compounds are taken. Substituting all these values into Eq.(10), one obtains the following relation between the parameters of cooperative interaction $J^{ls,ls} : J^{hs,ls} : J^{hs,hs} = 3.22 : 1.79 : 1$. As a consequence, in the subsequent analysis of the experimental data instead of three independent $J^{f,f'}$ parameters only $J^{ls,ls}$ can be used. At the same time it should be mentioned once more that these parameters are proportional to the square of the coefficient λ which plays the role of the phenomenological parameter of the model.

3.2. Effect of intracluster interactions on the spin transition in the tetranuclear squares

In this subsection the effect of the parameters δ_s and δ_d characterizing the interaction between SCO ions belonging to the same square will be examined. Since compounds containing SCO Fe^{II} (d^6) ions represent the object of our study, g_{ls} in all equations is set to 1 and g_{hs} is 15.

Later on, instead of the crystal field gap Δ, it is convenient to introduce the parameter $\Delta_{hl} = E^0_{hs,hs,hs,hs} - E^0_{ls,ls,ls,ls}$, where

$$E^0_{hs,hs,hs,hs} = \Delta - \frac{2\upsilon^2_{hs}}{\hbar\omega_{hs}}\left(1+\frac{J^{hs,ls}\upsilon_{ls}}{\hbar\omega_{ls}\upsilon_{hs}}\right)^2 + \sum_{p=1\ldots15} 2\hbar\omega^p_{hs} \qquad (16)$$

and

$$E^0_{ls,ls,ls,ls} = -\frac{2\upsilon^2_{ls}}{\hbar\omega_{ls}}\left(1+\frac{J^{ls,ls}}{\hbar\omega_{ls}}\right)^2 + \sum_{p=1\ldots15} 2\hbar\omega^p_{ls} \qquad (17)$$

can be easily obtained from Eqs.(8), (9) and represent the electron-vibrational energies of the tetranuclear cluster at low temperatures, when only the ground level with $k^p_l = 0$ (l = 1…4, p = 1…15) is populated and $\overline{\tau^{ls}x^{ls}} = -\frac{\upsilon_{ls}}{\hbar\omega_{ls}}$ and $\overline{\tau^{hs}x^{hs}} = 0$. In fact the gap Δ_{hl} represents the difference in the energies between the zero vibrational levels of the ground (*ls*) and upper (*hs*) electronic states of the whole tetranuclear cluster.

The effect of the parameters δ_s and δ_d characterizing the intracluster interactions on the spin transition in tetranuclear square complexes is illustrated in Figs.2 and 3, respectively. When both parameters are negligible, one-step transition occurs. The negative values of both parameters shift configurations with n = 1, 2 or 3 ions in the *hs*-state to the higher energies. As a consequence, the thermal populations of these configurations decrease thus increasing the relative population of the configuration with all ions in the *hs* state. The corresponding transition becomes more abrupt. The positive values of δ_s and δ_d parameters result in the opposite effect. The energy stabilization of configurations with n = 1, 2 or 3 makes the spin transition more gradual. At some positive values of these parameters a second step in the transition appears with the plateau between steps.

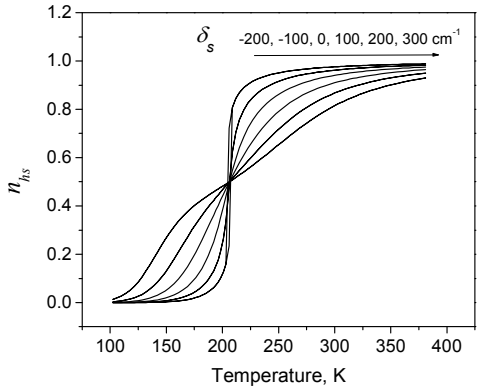

Fig.2. The population n_{hs} of the *hs*-state as a function of temperature calculated with Δ_{hl}=5000 cm^{-1}, δ_d=0, $J^{ls,ls}$ = 2.54 cm^{-1} and different δ_s.

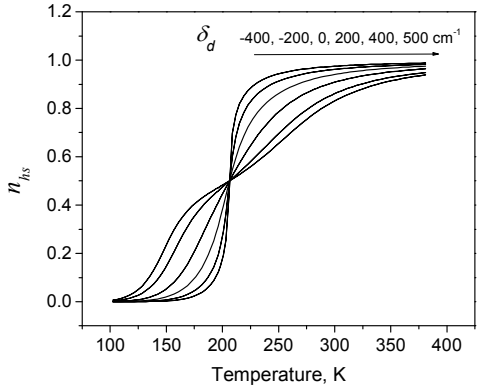

Fig.3. The population n_{hs} of the *hs*-state as a function of temperature calculated with Δ_{hl}=5000 cm^{-1}, δ_s=0, $J^{ls,ls}$ = 2.54 cm^{-1} and different δ_d.

Comparison of Figs 2 and 3 shows that the same type curve can be obtained for a larger value of the δ_d parameter than that of δ_s. However, the most important distinction between the effects of these two parameters is in their action on the configurations with *n* = 2 (two *hs* and two *ls* Fe ions in the cluster). As can be seen from Eq.(14), the δ_d parameter affects only the cluster configuration with two *hs* ions located along the side of the square, while the δ_s parameter has a stronger effect on the cluster configuration with two *hs* ions located along the diagonal of the square. As a result, the indistinct plateau between the two steps in Fig.2 corresponds to the configuration with two *hs* ions located along the diagonal of the square, while in Fig.3 a similar plateau is due to the configuration with two *hs* ions located along the side of the square. In Figs 4 and 5 the thermal variation of the populations n_0, n_1, n_2^s, n_2^d, n_3, n_4 of the energy levels

corresponding to the configurations of the cluster illustrated in Fig.1 is given for the cases δ_d=0, δ_s = 300 cm^{-1}, and δ_d = 500 cm^{-1}, δ_s=0, respectively.

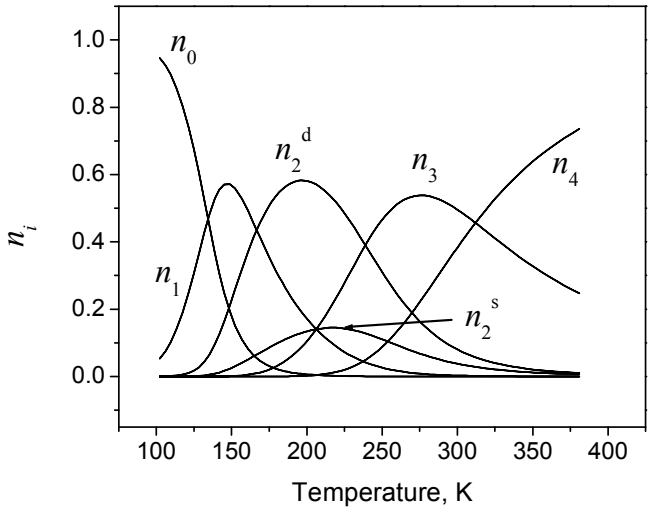

Fig.4. Thermal variation of the populations of the energy levels corresponding to cluster configurations illustrated in Fig.1 in the case of Δ_{hl}=5000 cm^{-1}, δ_s=300 cm^{-1}, δ_d=0 and $J^{ls,ls}$ = 2.54 cm^{-1}.

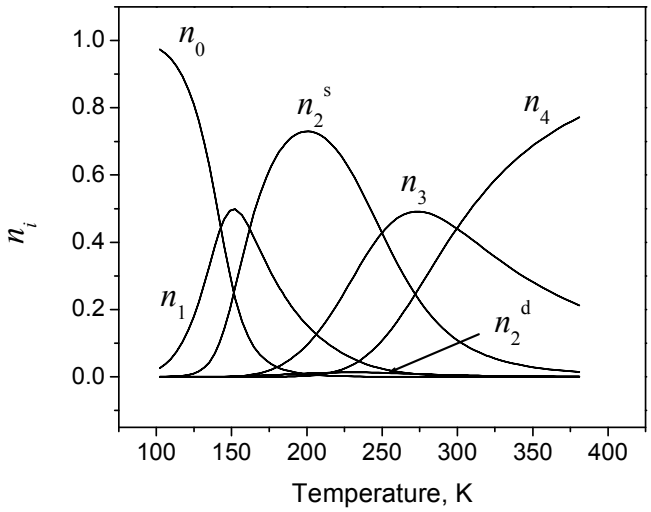

Fig.5. Thermal variation of the populations of the energy levels corresponding to cluster configurations illustrated in Fig.1 in the case of Δ_{hl}=5000 cm^{-1}, δ_s=0, δ_d=500 cm^{-1} and $J^{ls,ls}$ = 2.54 cm^{-1}.

Figures 4 and 5 clearly show that at low temperatures in the majority of clusters all four ions are in the *ls*-state, while at high temperatures the clusters with all four ions in the *hs*-state dominate. It can be indicated as well a range of temperatures wherein the number of clusters in the states with two *hs*- and two *ls*- ions significantly exceeds the number of clusters in other configurations. This fact explains the presence of the plateau in the temperature dependence of the *hs* –fraction.

3.3. Spin crossover in [Fe(tpa){N(CN)$_2$}]$_4$·(BF$_4$)$_4$·(H$_2$O)$_2$ compound

In this section the model presented above is applied for the description of the two-step spin transition in the [Fe(tpa){N(CN)$_2$}]$_4$·(BF$_4$)$_4$·(H$_2$O)$_2$ compound. Synthesis, crystal structure and magnetic behavior of this compound are presented in [21]. The compound undergoes a two-step spin transition with critical temperatures of 194 and 302 K, respectively. The analysis of the bond lengths at 250 K indicates that at this temperature two of the four Fe^{II} ions are in the *ls* -configuration and two others are in the *hs* one, with ions in the identical electronic configuration being along the diagonal of the square. Figures 6 and 7 present the results of calculation of the magnetic susceptibility and the population of the *hs*-state as functions of temperature. The best fit parameters are parts of the Figures captions. The values of the δ_n^i parameters determined by Eq.(14) are δ_1= 120 cm^{-1}, δ_2^s= -40 cm^{-1}, δ_2^d = 560 cm^{-1}, δ_3= 120 cm^{-1}. For this set of parameters the most significant stabilization takes place for the cluster configuration with 2 *hs* ions along the diagonal of the square as it is observed in [21]. The energy stabilization of configurations with one or three *hs* ions is much smaller while the cluster configuration with 2 *hs* ions along the side of the square becomes higher in energy. As a result, the configuration with 2 *hs* ions along the diagonal of the square gives the dominant contribution to the magnetic susceptibility (Fig.8) in the area of the plateau observed between the two steps of the experimental curve that agrees with the experimental data on the structure of the [Fe(tpa){N(CN)$_2$}]$_4$·(BF$_4$)$_4$·(H$_2$O)$_2$ complex.[21] The calculated *hs*-fraction presented in Fig.7 demonstrates a two-step spin transition as well. The main contribution of the configuration with two *hs*-ions situated on the diagonal to the χT product in the range of its plateau is also confirmed by the populations of the energy states corresponding to all cluster configurations (Fig.1) calculated with the best fit parameters (Fig.8). From Fig.8 it follows that at temperatures 200-300 K the population of the energy levels arising from the cluster configurations with two

hs-ions situated along the diagonal of the square significantly exceeds the populations of levels originating from all other configurations.

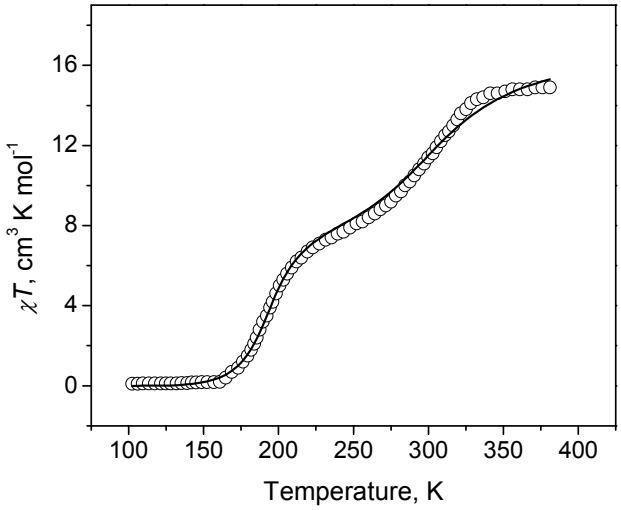

Fig.6. Experimental χT vs. T dependence for $[Fe(tpa)\{N(CN)_2\}]_4 \cdot (BF_4)_4 \cdot (H_2O)_2$ (open circles)[21] and the theoretical curve calculated with Δ_{hl}=5800 cm^{-1}, δ_e=280 cm^{-1}, δ_d=-320 cm^{-1}, $J^{ls,ls}$ = 2.46 cm^{-1} and g=2.37.

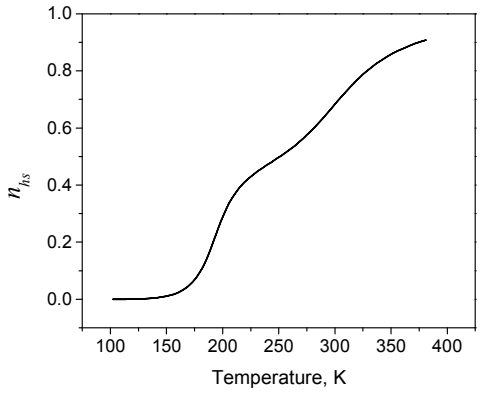

Fig.7. n_{hs} vs. T dependence for $[Fe(tpa)\{N(CN)_2\}]_4 \cdot (BF_4)_4 \cdot (H_2O)_2$ compound calculated with Δ_{hl} =5800 cm^{-1}, δ_e=280 cm^{-1}, δ_d=-320 cm^{-1} and $J^{ls,ls}$ = 2.46 cm^{-1}.

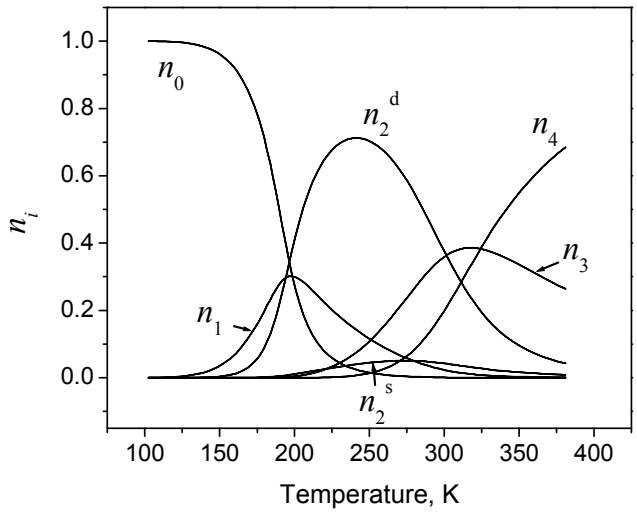

Fig.8. Thermal variation of the populations of the energy levels arising from different configurations of the $[Fe(tpa)\{N(CN)_2\}]_4\cdot(BF_4)_4\cdot(H_2O)_2$ cluster calculated with the parameters Δ_{hl}=5800 cm^{-1}, δ_e=280 cm^{-1}, δ_d=-320 cm^{-1} and $J^{ls,ls}$ = 2.46 cm^{-1}.

It is seen that the presented above model nicely describes the two-step spin transition observed in the $[Fe(tpa)\{N(CN)_2\}]_4\cdot(BF_4)_4\cdot(H_2O)_2$ cluster compound.[21] The obtained value of Δ_{hl} is reasonable and it is of the order of typical values for spin crossover compounds. As to the parameters of cooperative interaction in fact in the examined problem the role of these parameters play the products $J^{ls,ls}\,\overline{\tau^{ls}x^{ls}}$, $J^{hs,ls}\,\overline{\tau^{hs}x^{hs}}$, $J^{hs,ls}\,\overline{\tau^{ls}x^{ls}}$, $J^{hs,hs}\,\overline{\tau^{hs}x^{hs}}$ which magnitudes are of the same order as the transition temperatures. This result can be explained as follows. In the previous models of SCO (see, for instance, Refs [47,48]) the order parameter represents the mean value of the electronic matrix $\hat{\tau}_{ni}$ connected with the matrices $\hat{\tau}_{hs}^{ni}$ and $\hat{\tau}_{ls}^{ni}$ by the relations $\hat{\tau}_{hs}^{ni}=\frac{1}{2}(1+\tau_{ni}),\ \hat{\tau}_{ls}^{ni}=\frac{1}{2}(1-\tau_{ni})$. Therefore, the thermal average of τ_{ni} takes on the values in the range between -1 and 1. At the same time in the present model the role of the order parameters is played by the mean values of the products of the electronic matrices $\hat{\tau}_{hs}^{ni}$ and $\hat{\tau}_{ls}^{ni}$ and the vibrational coordinates x^{hs} and x^{ls}, respectively. These products can acquire the values much higher than 1 because the mean values of the vibrational coordinates x^{hs} and x^{ls} approximately correspond to the minima of the adiabatic potential sheets in the *hs*- and *ls*-states

and can be simply expressed through the vibronic coupling constants υ_{hs} and υ_{ls}. A more detailed explanation of this fact can be found in our paper.[58]

4. Concluding remarks

In this paper we have presented a new microscopic approach to the problem of SCO in crystals containing polynuclear clusters as structural units. It should be underlined that the developed approach has no limitations on the number of spin crossover ions in each cluster and can be applied to crystals containing clusters of different nuclearities and geometries. Moreover, the approach allows to examine clusters with different origins of intracluster interactions. These interactions lead to interesting peculiarities in the magnetic characteristics of bi- and polynuclear clusters not observed in mononuclear molecular crystals. The cornerstone of the developed approach is the account for the interaction of SCO ions both with the local and acoustic crystal lattice vibrations. The participation of each SCO ion in both named vibrations gives rise to the cooperative interaction between all SCO ions in the crystal. For the first time this type of cooperativity was accounted for in papers [58,59] aimed at the examination of spin crossover in crystals containing mono- and binuclear clusters. In the present paper the Hamiltonian of cooperative interaction is generalized to the case of polynuclear cluster compounds. In order to demonstrate the applicability of the developed approach, SCO in tetranuclear square cluster compounds was examined. It is demonstrated that the intracluster interactions between SCO ions in systems of this type can be described with the aid of 2 parameters $\delta_{s(d)} = U_{hshs}^{s(d)} + U_{lsls}^{s(d)} - 2U_{hsls}^{s(d)}$ characterizing the interaction of two SCO ions situated along the side or the diagonal of the square. The influence of these parameters on the type of the SCO transition in tetranuclear squares has been elucidated. It has been demonstrated that in tetranuclear square complexes at definite values of the parameters $\delta_{s(d)}$ a two-step spin transition can be observed. The interplay between these parameters determines whether the plateau between two steps in the temperature dependence of the magnetic susceptibility corresponds to the location of 2 *hs* ions along the side or the diagonal of the square.

In the framework of the developed approach the two-step spin transition observed in the $[Fe(tpa)\{N(CN)_2\}]_4\cdot(BF_4)_4\cdot(H_2O)_2$ compound has been described. The main features of the SCO phenomenon in this system, including the plateau between the steps corresponding to the cluster configuration with 2 *hs* ions along the diagonal of the square, have been reproduced.

Acknowledgement

SK and SO are grateful to Science and Technology Center in Ukraine (STCU) for financial support (project N 6219). AP acknowledges support from the Ministry of Education and Science of Russian Federation (Agreement No. 14.W03.31.0001 – Institute of Problems of Chemical Physics of the Russian Academy of Sciences, Chernogolovka). The support of the Ministry of Education, Culture and Research of Moldova (project 15.817.02.06F) is also highly appreciated.

1931) *Iron dithiocarbamates and nitroso dithiocarbamates*. Atti Accad. Lincei 13, 809–813.

References

[1] Cambi L., Cagnasso A., Iron dithiocarbamates and nitroso dithiocarbamates . *Atti Accad. Naz. Lincei* **1931**, *13*, 809-813.

[2] Cambi L., Szego L., Über die magnetische Susceptibilität der komplexen Verbindungen. *Ber. Dtsch. Chem. Ges. B* **1931**, *64*, 2591−2598.

[3] Cambi L., Szego L., Über die magnetische Susceptibilität der komplexen Verbindungen (II. Mittel.). *Ber. Dtsch. Chem. Ges. B* **1933**, *66*, 656−661.

[4] Cambi L., Malatesta, L., Magnetismus und Polymorphie innerer Komplexsalze:Eisensalze der Dithiocarbamidsäuren. *Ber.Dtsch.Chem.Ges* (A and B series) **1937**, *70*, 2067-2078.

[5] Sanvito S., Molecular spintronics, *Chem. Soc. Rev*., **2011**, *40*, 3336-3355.

[6] Gamez P., Sanchez Costa J., Quesada M., Aromi G., Iron Spin-Crossover compounds: from fundamental studies to practical applications, *Dalton Trans.,* **2009**, 7845-7853.

[7] Letard J.-F., Guionneau P., Goux-Capes L., Towards Spin Crossover Applications, *Top. Curr. Chem.* **2004**, *235*, 221-249.

[8] Kahn O., Martinez C. J., Spin-Transition Polymers: From Molecular Materials Toward Memory Devices, *Science* **1998**, *279*, 44-48.

[9] Kahn O., Launey J. P., Molecular bistability; an overview, *Chemtronics* **1988**, *3*, 140-151.

[10] Kahn O., Krober J., Jay C., Spin Transition Molecular Materials for displays and data recording, *Adv. Mater*., **1992**, *4*, 718-728.

[11] Ruiz E., Charge transport properties of spin crossover systems, *Phys. Chem. Chem. Phys*. **2014**, *16*, 14-22.

[12] Gütlich P., Goodwin H.A. (Eds.). Spin Crossover in Transition Metal Compounds I-III. Berlin and Heidelberg: Springer-Verlag, **2004** (*Top. Curr. Chem*. **2004**, 233-235).

[13] Gütlich, P. Spin Crossover – Quo Vadis?, *Eur. J. Inorg. Chem*. **2013**, 581-591.

[14] Decurtins S., Gütlich P., Köhler C.P., Spiering H. New Examples of Light-induced Excited Spin State Trapping (LIESST) in Iron(II) Spin-crossover Systems, *J. Chem. Soc., Chem. Commun.* **1985**, 430-432.

[15] Real J. A., Bolvin H., Bousseksou A., Dworkin A., Kahn O., Varret F., Zarembowitch J. Two-Step Spin Crossover in the New Dinuclear Compound $[Fe(bt)(NCS)_2]_2$bpym, with bt = 2,2′-bi-2-Thiazoline and bpym = 2,2′-Bipyrimidine: Experimental Investigation and Theoretical Approach. *J. Am. Chem. Soc*. **1992**, *114*, 4650−4658.

[16] Bousseksou A., Molnar G., Real J. A., Tanaka K. Spin Crossover and Photomagnetism in Dinuclear Iron(II) Compounds. *Coord. Chem. Rev*. **2007**, *251*, 1822−1833.

[17] Gütlich P., Garcia Y. In Mössbauer Spectroscopy, Yoshida Y., Langouche G., Eds.; Springer-Verlag: Berlin, Heidelberg, Germany, **2013**; 23−89.

[18] Wu D.-Y. Sato O., Einaga Y., Duan C.-Y., A Spin-Crossover Cluster of Iron(II) Exhibiting a Mixed-Spin Structure and Synergy between Spin Transition and Magnetic Interaction, *Angew. Chem. Int. Ed*. **2009**, *48*, 1475 –1478.

[19] Nihei M., Ui M., Yokota M., Han L., Madda A., Kishida H., Okamoto H., Oshio H., Two-Step Spin Conversion in a Cyanide-Bridged Ferrous Square, *Angew. Chem. Int. Ed*. **2005**, *44*, 6484 – 6487.

[20] Matsumoto T., Newton G. N., Shiga T., Hayami S., Matsui Y., Okamoto H., Kumai R., Murakami Y., Oshio H., Programmable spin-state switching in a mixed-valence spin-crossover iron grid, *Nature Commun*. **2014**, *5*, 3865.

[21] Wei R.-J., Huo Q., Tao J., Huang R.-B., Zheng L.-S., Spin-Crossover Fe^{II}_4 Squares: Two-Step Complete Spin Transition and Reversible Single-Crystal-to-Single-Crystal Transformation, *Angew. Chem. Int. Ed*. **2011**, *50*, 8940-8943.

[22] Steinert M.,Schneider B., Dechert,S, Demeshko,S., Meyer,F., Spin-State Versatility in a Series of Fe_4[2x2] Grid Complexes: Effects of Counteranions,Lattice Solvent and Intramolecular Cooperativity, *Inorganic Chemistry*. **2016**, *55*, 2363-2373.

[23] Dhers,S.,Mondal,A., Aguilà,D., Ramirez,J., Vela,S., Dechambernoit,P., Rouziérs, M., Nitschke,J.R., Clérac R.,J.-M. Lehn, Spin State Chemistry: Modulation of Ligand pK_a by Spin State Switching in a [2x2] Iron(II) Grid=Type Complex, *JACS* **2018**, *140*, 8218-8227.

[24] Spiering H., Elastic Interaction in Spin-Crossover Compounds, *Top. Curr. Chem.* **2004**, *235*, 171-195.

[25] Spiering H., Meissner E., Koppen H., Muller E. W., Gutlich P., The effect of the lattice expansion on high spin ↔ low spin transitions, *Chem. Phys*. **1982**, *68*, 65-71.

[26] Spiering H., Boukheddaden K., Linares J., Varret F., Total free energy of a spin-crossover molecular system, *Phys. Rev. B* **2004**, *70*, 184106 (15 pages).

[27] Wajnflasz J., Pick R., Transitions «Low Spin»-«High Spin» Dans Les Complexes De Fe^{2+}, *J. Phys. Colloq*. **1971**, *32*, C1-91.

[28] Bousseksou A., Nasser J., Linares J., Boukheddaden K., Varret F., Ising-like model for the two-step spin-crossover, *J. Phys. I* (France), **1992**, *2*, 1381-1404.

[29] Bousseksou A., Varret F., Nasser J., Ising-like model for the two step spin-crossover of binuclear molecules, *J. Phys. I* (France), **1993**, *3*, 1463-1474.

[30] Bousseksou A., Constant-Machado H., Varret F., A Simple Ising-Like Model for Spin Conversion Including Molecular Vibrations, *F. J. Phys. I* (France), **1995**, *5*, 747-749.

[31] Boukheddaden K., Shteto I., Hôo B., Varret F., Dynamical model for spin-crossover solids. I. Relaxation effects in the mean-field approach, *Phys. Rev. B*, **2000**, *62*, 14796-14805.

[32] Boukheddaden K., Shteto I., Hôo B., Varret F., Dynamical model for spin-crossover solids. II. Static and dynamic effects of light in the mean-field approach, *Phys. Rev. B*, **2000**, *62*, 14806-14817.

[33] Nishino M., Miyashita S., Boukheddaden K., Effective interaction range in the spin crossover phenomenon: Wajnflasz and domain models, *J. Chem. Phys*., **2003**, *118*, 4594 (4 pages).

[34] Nishino M., Boukheddaden K., Miyashita S., Varret F., Dynamical aspects of photoinduced magnetism and spin-crossover phenomena in Prussian blue analogs, *Phys. Rev. B*, **2005**, *72*, 064452 (7 pages).

[35] Miyashita S., Konishi Y., Tokoro H., Nishino M., Boukheddaden K., Varret F., Structures of Metastable States in Phase Transitions with a High-Spin Low-Spin Degree of Freedom, *Prog. Theor. Phys.*, **2005**, *114*, 719-735.

[36] Chiruta D., Linares J., Garcia Y., Dahoo P. R., Dimian M., Analysis of the Hysteretic Behaviour of 3D Spin Crossover Compounds by Using an Ising-Like Model, *Eur. J. Inorg. Chem.* **2013**, 3601-3608.

[37] Atitoaie A., Tanasa R., Stancu A., Enachescu C., Study of spin crossover nanoparticles thermal hysteresis using FORC diagrams on an Ising-like model, *J. Magn. Magn. Mater*. **2014**, *368*, 12-18.

[38] Nicolazzi W., Pavlik J., Bedoui S., Molnar G., Bousseksou A., Elastic Ising-like model for the nucleation and domain formation in spin crossover molecular solids, *Eur. Phys. J.: Spec. Top.* **2013**, *222*, 1137-1159.

[39] Nasser J. A., Boukheddaden K., Linares J., Two-step spin conversion and other effects in the atom-phonon coupling model, *Eur. Phys. J. B* **2004**, *39*, 219-227.

[40] Rotaru A., Linares J., Codjovi E., Nasser J., Stancu A., Size and pressure effects in the atom-phonon coupling model for spin crossover compounds, *J. Appl. Phys.* **2008**, *103*, 07B908.

[41] Boukheddaden K., Miyashita S., Nishino M., Elastic interaction among transition metals in one-dimensional spin-crossover solids, *Phys. Rev B* **2007**, *75*, 094112.

[42] Boukheddaden K., Static and Dynamical Aspects of a Phonon-Induced Spin-Crossover Transition – Local Equilibrium Approach, *Eur. J. Inorg. Chem*. **2013**, 865-874.

[43] Enachescu C., Stoleriu L., Stancu A., Hauser A., Model for Elastic Relaxation Phenomena in Finite 2D Hexagonal Molecular Lattices, *Phys. Rev. Lett.* **2009**, *102*, 257204.

[44] Nishino M., Boukheddaden K., Miyashita S., Molecular dynamics study of thermal expansion and compression in spin-crossover solids using a microscopic model of elastic interactions, *Phys. Rev. B* **2009**, *79*, 012409.

[45] Nasser J. A., Chassagne L., S. Topçu, Linares J., Alayli A., Study of the atom-phonon coupling model for (SC) partition function: first order phase transition for an infinite linear chain, *Eur. Phys. J. B* **2014**, *87*, 69.

[46] Chakraborty P., Enachescu C., Hauser A., Analysis of the Experimental Data for Pure and Diluted $[Fe_xZn_{1-x}(bbtr)_3](ClO_4)_2$ Spin-Crossover Solids in the Framework of a Mechanoelastic Model, *Eur. J. Inorg. Chem.* **2013**, 770-780.

[47] Klokishner S., Linares J., Varret F., Effect of hydrostatic pressure on phase transitions in spin-crossover 1D systems, *Chem. Phys*. **2000**, *255*, 317-323.

[48] Klokishner S., Linares J., Effects of Intra- and Intercenter Interactions in Spin Crossover: Application of the Density Matrix Method to the Nonequilibrium Low-Spin↔High-Spin Transitions Induced by Light, *J. Phys. Chem. C* **2007**, *111*, 10644-10651.

[49] Klokishner S., Roman M., Reu O., A Model of Spin Crossover in Manganese(III) Compounds: Effects of Intra- and Intercenter Interactions, *Inorg. Chem*. **2011**, *50*, 11394-11402.

[50] Ostrovsky S. M., Reu O. S., Palii A. V., Clemente-Leon M., Coronado E., Waerenborgh J. C., Klokishner S. I., Modeling the Magnetic Properties and Mössbauer Spectra of Multifunctional Magnetic Materials Obtained by Insertion of a Spin-Crossover Fe(III) Complex into Bimetallic Oxalate-Based Ferromagnets, *Inorg. Chem*. **2013**, *52*, 13536-13545.

[51] Klokishner S., Ostrovsky S., Palii A., Shatruk M., Funck K., Dunbar K., Tsukerblat B., Vibronic Model for Cooperative Spin-Crossover in Pentanuclear $\{[M^{III}(CN)_6]_2[M'^{II}(tmphen)_2]_3\}$ (M/M' = Co/Fe, Fe/Fe) Compounds, *J. Phys. Chem. C* **2011**, *115*, 21666-21677.

[52] Roman M. A., Reu O. S., Klokishner S. I., Charge-Transfer-Induced Spin Transitions in Crystals Containing Cyanide-Bridged Co–Fe Clusters: Role of Intra- and Intercluster Interactions, *J. Phys. Chem. A* **2012**, *116*, 9534-9544.

[53] Ostrovsky S., Palii A., Klokishner S., Shatruk M., Funck K., Achim C., Dunbar K.R., Tsukerblat B., Vibronic Approach to the Cooperative Spin Transitions in Crystals Based on Cyano-Bridged Pentanuclear M_2Fe_3 (M=Co, Os) Clusters, *Prog. Theor. Chem. Phys.* **2012**, *23*, 379-396.

[54] Kambara T., The Effect of Iron Concentration on the High-Spin ↔ Low-Spin Transitions in Iron Compounds, *J. Phys. Soc. Jpn*, **1980**, *49*, 1806-1811.

[55] Sasaki N., Kambara T., Theory of cooperative high-spin ↔ low-spin transitions in iron (III) compounds induced by the molecular distortions, *J. Chem. Phys.*, **1981**, *74*, 3472-3481.

[56] Sasaki N., Kambara T., Theory of the two-step spin conversion induced by the cooperative molecular distortions in spin-crossover compounds, *Phys. Rev. B*, **1989**, *40*, 2442-2449.

[57] Pavlik J., Boča R., Established Static Models of Spin Crossover, *Eur. J. Inorg. Chem*. **2013**, 697-709.

[58] Palii A., Ostrovsky S., Reu O., Tsukerblat B., Decurtins S., Liu S.-X., Klokishner S., Microscopic Theory of Cooperative Spin Crossover: Interaction of Molecular Modes with Phonons, *J. Chem. Phys*. **2015**, *143*, 084502 (12 pages).

[59] Palii A., Ostrovsky S., Reu O., Tsukerblat B., Decurtins S., Liu S.-X., Klokishner S., Diversity of Spin Crossover Transitions in Binuclear Compounds: Simulation by Microscopic Vibronic Approach, *J. Phys. Chem. C* **2016**, *120*, 14444-14453.

[60] Hizhnyakov V., Pae K., Vaikjarv T., Optical Jahn–Teller effect in the case of local modes and phonons, *Chem. Phys. Lett*. **2012**, *525-526*, 64-68.

[61] Pae K., Hizhnyakov V., Nonadiabaticity in a Jahn-Teller system probed by absorption and resonance Raman scattering, *J. Chem. Phys.* **2013**, *138*, 104103.

[62] Pae K., Hizhnyakov V., Quantum friction of pseudorotation in Jahn-Teller System: Passage through conical intersection, *J. Chem. Phys.* **2016**, *145*, 064108.

[63] Van Vleck H., Paramagnetic Relaxation Times for Titanium and Chrome Alum, *Phys. Rev*. **1940**, *57*, 426.

[64] Malkin B. Z., Ion-Phonon Interactions, in: Liu, G., Jacquier, B. (Eds.), Spectroscopic Properties of Rare Earths in Optical Materials, Springer, Berlin, **2005**, v. *83*, 130−190.

[65] Blaja M. G., Vylegzhanin D. N., Kaminskii A. A., Klokishner S. I., Perlin Yu. E., The Determination of Crystal Phonon Density on Vibrational Satellites of Zero-Phonon Lines in Luminescence Spectra of TR^{3+} Ions, *Bull. Acad. Sci. USSR: Phys. Ser.* **1976**, *40*, 69.

[66] Jung J., Spiering H., Yu Z., Gütlich P., The debye-waller factor in spincrossover molecular crystals: a mössbauer study on $[Fe_xZn_{1-x}(ptz)_6]$, *Hyperfine Interactions* **1995**, *95*, 107-128.

[67] Ronayne K.L., Paulsen H., Höfer A., Dennis A.C., Wolny J.A., Chumakov A.I., Schünemann V., Winkler H., Spiering H., Bousseksou A., Gütlich P., Trautwein A.X.

McGarvey J.J., Vibrational spectrum of the spin crossover complex $[Fe(phen)_2(NCS)_2]$ studied by IR and Raman spectroscopy, nuclear inelastic scattering and DFT calculations, *Phys. Chem. Chem. Phys*. **2006**, *8*, 4685-4693.

[68] Jung,J; Schmitt,G.; Wiehl,L.; Hauser,A.; Knorr,K.; Spiering ,H.; Gütlich,P. The cooperative spin transition in $[Fe_xZn_{1-x}(ptz)_6](BF_4)_2$: II. Structural properties and calculation of the elastic interaction, *Z. Phys. B* **1996**, *100*, 523 -534.

(Sophia Klokishner- ORCID 0000-0003-2837-4592)

(Palii Andrew- ORCID 0000-0002-1682-2362)

(Shi-Xia Liu- ORCID 0000-0001-6104-4320)

(Silvio Decurtins- ORCID 0000-0002-1624-8217)

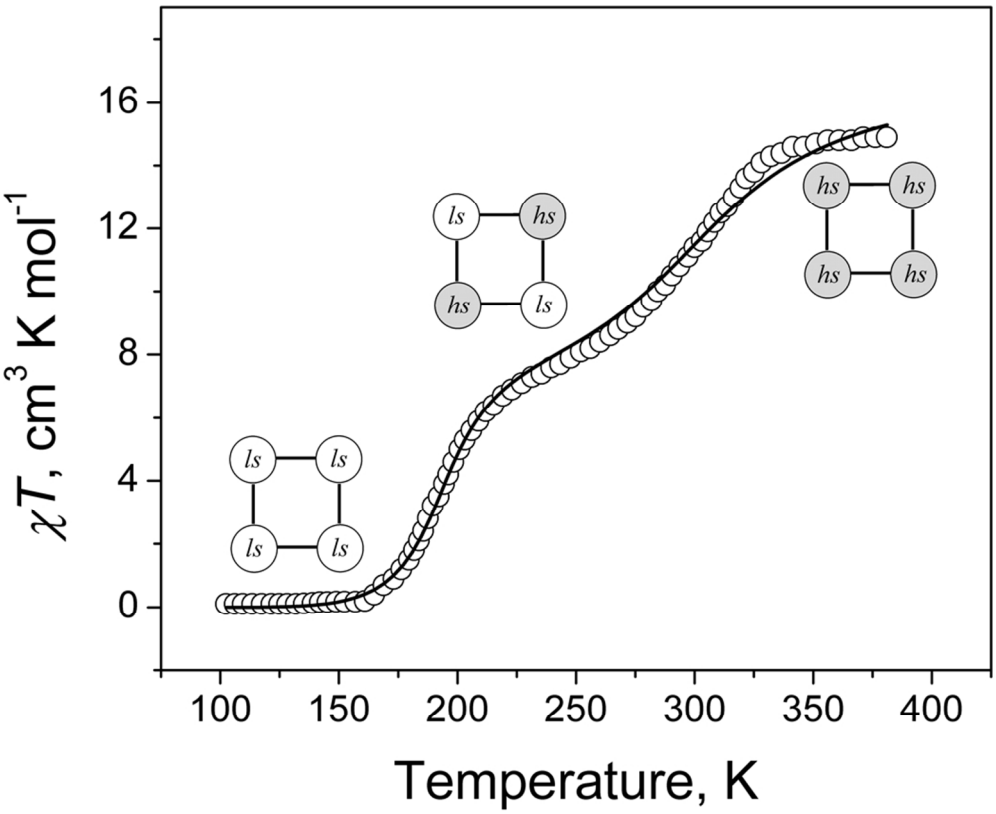

178x146mm (150 x 150 DPI)